Electronic Properties of the Linear Antiferromagnetically Coupled Clusters $[Fe_3S_4(SR)_4]^{3-}$, Structural Isomers of the $[Fe_3S_4]^+$ Unit in Iron-Sulfur Proteins

J.-J. Girerd,[1a,b] G. C. Papaefthymiou,[1c] A. D. Watson,[1a] E. Gamp,[1d] K. S. Hagen,[1a] N. Edelstein,[1d] R. B. Frankel,[1c] and R. H. Holm*[1a]

Contribution from the Department of Chemistry, Harvard University, Cambridge, Massachusetts 02138, the Laboratoire de Spectrochimie des Éléments de Transition, ERA CNRS 672, Université de Paris-Sud, F-91405 Orsay, France, the Francis Bitter National Magnet Laboratory, Massachusetts Institute of Technology, Cambridge, Massachusetts 02139, and the Materials and Molecular Research Division, Lawrence Berkeley Laboratory, Berkeley, California 94720. *Received March 6, 1984*

Abstract: The magnetic susceptibility, magnetization, and Mössbauer spectroscopic properties of the trinuclear clusters $[Fe_3S_4(SR)_4]^{3-}$ (R = Et, Ph), containing the linear $[Fe(\mu_2\text{-}S)_2Fe(\mu_2\text{-}S)_2Fe]^+$ core with Fe···Fe separations of 2.71 Å, have been examined in order to characterize this unique magnetic system. $(Et_4N)_3[Fe_3S_4(SEt)_4]$ follows the Curie–Weiss law $\chi^M = 4.268/(T + 0.58)$ at 5–300 K, with the average magnetic moment of 5.84 μ_B corresponding to an $S = {}^5/_2$ ground state. The magnetization approaches $\mu = gS = 5$ μ_B per cluster at low temperature and provides an estimate of the zero-field splitting parameter $|D| \lesssim 1$ cm^{-1}. Mössbauer spectra reveal the presence of antiferromagnetically coupled, high-spin Fe(III) atoms. Close resemblance of spectra in the solid and in DMF solution demonstrates retention of the linear structure in solution. Two magnetic subsites in a 2:1 ratio are observed, with the more intense and less intense subsites corresponding to the hyperfine fields -310 ± 5 and $+230 \pm 5$ kOe, respectively. It is shown that from these values the hyperfine interaction constants $a/g_n\beta_n = -153 \pm 3$ and -137 ± 3 kOe/spin can be calculated for the more intense and less intense subsites, respectively. The more intense subsite, with the larger hyperfine interaction, corresponds to the two end Fe(III) atoms (1, 3), whose magnetic moments are parallel to each other and to the total moment of the cluster. The less intense subsite, with the smaller hyperfine interaction, is the central Fe(III) atom (2) whose moment is antiparallel to the cluster total moment and hence to the moments of the other two Fe(III) atoms. The estimates $J_{12} = J_{23}$ ca. -300 cm^{-1} and $-100 \lesssim J_{13} \lesssim 100$ cm^{-1} were obtained from susceptibility data. A theoretical treatment of three antiferromagnetically coupled $S = {}^5/_2$ spins shows that when $J_{12} = J_{23} \ll J_{13}$ the sextet ground state is stabilized. In the $[Fe_3S_4]^+$ sites of ferredoxins the ground state is $S = {}^1/_2$, corresponding to $J_{12} \cong J_{23} \cong J_{13}$. Thus the linear $[Fe_3S_4]^+$ core of $[Fe_3S_4(SR)_4]^{3-}$ is a structural isomer of the protein site. Alternative site structures based on tetrahedral coordination and Fe···Fe separations of ~2.7 Å are presented, and existing topological equivalents of these structures are noted. The linear structure has recently been shown to occur in an unfolded form of aconitase.

The means of formation, geometrical and electronic structures, and physiological function (if any) of the recently discovered 3-Fe sites in proteins provide some of the principal matters for investigation in contemporary iron–sulfur biochemistry. The present state of understanding of these sites has been incisively reviewed.[2] The 3-Fe sites in *Azotobacter vinelandii* ferredoxin (*Av* Fd I),[3-7] *Desulfovibrio gigas* (*Dg* Fd II),[8-14] and the inactive form of the Krebs cycle enzyme beef heart aconitase[15-19] have been the most thoroughly examined. These sites are, however, of substantially wider occurrence.[2]

Crystallographic studies of *Av* Fd I have led to identification of the 3-Fe site as $[Fe_3S_3(S\text{-}Cys)_5(oxo)]$.[3] This entity contains a cyclic $[Fe_3(\mu_2\text{-}S)_3]^{3+}$ core with a Fe···Fe mean separation of 4.1 Å, distorted tetrahedral coordination at the Fe(III) atoms, and an unidentified oxygen ligand. EXAFS results for and chemical analysis of *Dg* Fd II[12,14] and aconitase[17] clearly demonstrate a different site composition (Fe_3S_4) and structure. The mean Fe···Fe separations of ~2.7 Å point to a compact, cluster-type structure in the $[Fe_3S_4]^+$ cores of the oxidized forms of these proteins. The essential structure in *Dg* Fd II[12] appears to be retained upon reduction to $[Fe_3S_4]^0$, an oxidation level observed for all Fe_3S_4 sites.[2] Further, resonance Raman spectral properties of crystalline and frozen solution samples of *Av* Fd I, obtained subsequent to the X-ray diffraction work,[3] have been interpreted in terms of a Fe_3S_4 site.[7] At least by this spectral criterion, the structure of this site is closely similar to that in aconitase.[16]

(1) (a) Harvard University. (b) University of Paris. (c) Massachusetts Institute of Technology. (d) Lawrence Berkeley Laboratory.

(2) Beinert, H.; Thomson, A. J. *Arch. Biochem. Biophys.* **1983**, *222*, 333.

(3) (a) Ghosh, D.; Furey, W., Jr.; O'Donnell, S.; Stout, C. D. *J. Biol. Chem.* **1981**, *256*, 4185. (b) Ghosh, D.; O'Donnell, S.; Furey, W., Jr.; Robbins, A. H.; Stout, C. D. *J. Mol. Biol.* **1982**, *158*, 73. (c) Howard, J. B.; Lorsbach, T. W.; Ghosh, D.; Melis, K.; Stout, C. D. *J. Biol. Chem.* **1983**, *258*, 508.

(4) Emptage, M. H.; Kent, T. A.; Huynh, B. H.; Rawlings, J.; Orme-Johnson, W. H.; Münck, E. *J. Biol. Chem.* **1980**, *255*, 1793.

(5) Sweeney, W. V. *J. Biol. Chem.* **1981**, *256*, 12222.

(6) (a) Morgan, T. V.; Stephens, P. J.; Burgess, B. K.; Stout, C. D. *FEBS Lett.* **1984**, *167*, 137. (b) Morgan, T. V.; Stephens, P. J.; Devlin, F.; Stout, C. D.; Melis, K. A.; Burgess, B. K. *Proc. Natl. Acad. Sci. U.S.A.* **1984**, *81*, 1931.

(7) Johnson, M. K.; Czernuszewicz, R. S.; Spiro, T. G.; Fee, J. A.; Sweeney, W. V. *J. Am. Chem. Soc.* **1983**, *105*, 6671.

(8) Huynh, B. H.; Moura, J. J. G.; Moura, I.; Kent, T. A.; LeGall, J.; Xavier, A. V.; Münck, E. *J. Biol. Chem.* **1980**, *255*, 3242.

(9) Thomson, A. J.; Robinson, A. E.; Johnson, M. K.; Moura, J. J. G.; Moura, I.; Xavier, A. V.; LeGall, J. *Biochim. Biophys. Acta* **1981**, *670*, 93.

(10) Johnson, M. K.; Hare, J. W.; Spiro, T. G.; Moura, J. J. G.; Xavier, A. V.; LeGall, J. *J. Biol. Chem.* **1981**, *256*, 9806.

(11) (a) Kent, T. A.; Moura, I.; Moura, J. J. G.; Lipscomb, J. D.; Huynh, B. H.; LeGall, J.; Xavier, A. V.; Münck, E. *FEBS Lett.* **1982**, *138*, 55. (b) Moura, J. J. G.; Moura, I.; Kent, T. A.; Lipscomb, J. D.; Huynh, B. H.; LeGall, J.; Xavier, A. V.; Münck, E. *J. Biol. Chem.* **1982**, *257*, 6259.

(12) Antonio, M. R.; Averill, B. A.; Moura, I.; Moura, J. J. G.; Orme-Johnson, W. H.; Teo, B.-K.; Xavier, A. V. *J. Biol. Chem.* **1982**, *257*, 6646.

(13) Gayda, J.-P.; Bertrand, P.; Theodule, F.-X.; Moura, J. J. G. *J. Chem. Phys.* **1982**, *77*, 3387.

(14) Beinert, H. *Anal. Biochem.* **1983**, *131*, 373.

(15) Kent, T. A.; Dreyer, J.-L.; Kennedy, M. C.; Huynh, B. H.; Emptage, M. H.; Beinert, H.; Münck, E. *Proc. Natl. Acad. Sci. U.S.A.* **1982**, *79*, 1096.

(16) Johnson, M. K.; Czernuszewicz, R. S.; Spiro, T. G.; Ramsay, R. R.; Singer, T. P. *J. Biol. Chem.* **1983**, *258*, 12771.

(17) Beinert, H.; Emptage, M. H.; Dreyer, J.-L.; Scott, R. A.; Hahn, J. E.; Hodgson, K. O.; Thomson, A. J. *Proc. Natl. Acad. Sci. U.S.A.* **1983**, *80*, 393.

(18) Kennedy, M. C.; Emptage, M. H.; Dreyer, J.-L.; Beinert, H. *J. Biol. Chem.* **1983**, *258*, 11098.

(19) Emptage, M. H.; Dreyer, J.-L.; Kennedy, M. C.; Beinert, H. *J. Biol. Chem.* **1983**, *258*, 11106.

0002-7863/84/1506-5941$01.50/0

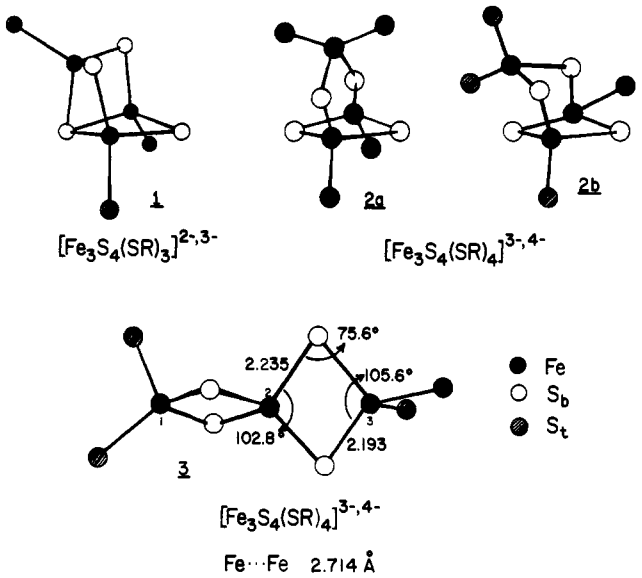

Figure 1. Candidate structures **1**, **2a**, **2b**, and **3** of protein Fe_3S_4 sites (b = bridging, t = terminal sulfur atom). Metric values for **3** apply to the R = Ph cluster under idealized D_{2d} symmetry.[23]

Diffraction-quality crystals of aconitase have been obtained,[20] but high-resolution structural results are not yet available.

With the exception of the Fe_3S_3 site in the original crystallographic samples of *Av* Fd I,[3] all structurally defined native[21,22] and synthetic[22-25] Fe–S–SR clusters containing at least one formal Fe(III) atom exhibit two especially prominent geometric features: (i) cores are, or are built up from bridged or fused, rhomboidal Fe_2S_2 groups within which the Fe···Fe separation is ~2.7 Å; (ii) all Fe atoms reside in (distorted) tetrahedral FeS_4 sites.[26] Imposition of one or both of these regularities on protein Fe_3S_4 sites leads to the candidate cluster structures[25] depicted in Figure 1; of these, **1** and **2** have also been put forward by others.[2,7,17] The C_{3v} structure **1** is a derivative of the familiar cubane-type Fe_4S_4 cluster obtained by removing one Fe atom. Structure **2** has two conformations, **2a** (C_{2v}) and "bent" **2b** (C_s). The latter approaches **1** and thus more nearly adheres to the desired Fe···Fe distance without undue angular deformation. This structure type departs from (i) to the extent that the top FeS_2 portion of the core is not part of a Fe_2S_2 rhomb. The D_{2d} structure **3** features a linear arrangement of Fe atoms, with two Fe_2S_2 groups bridged by a common Fe atom. The net charges on each structure indicate potential existence of two core oxidation levels, $[Fe_3S_4]^{+,0}$. In *Dg* Fd II[27] (6) and aconitase[28] (12) the indicated number of cysteinyl residues is more than sufficient to provide the terminal ligands in **1–3**. This is also the case with *Av* Fd I[3c] (9), which additionally contains one Fe_4S_4 cluster.

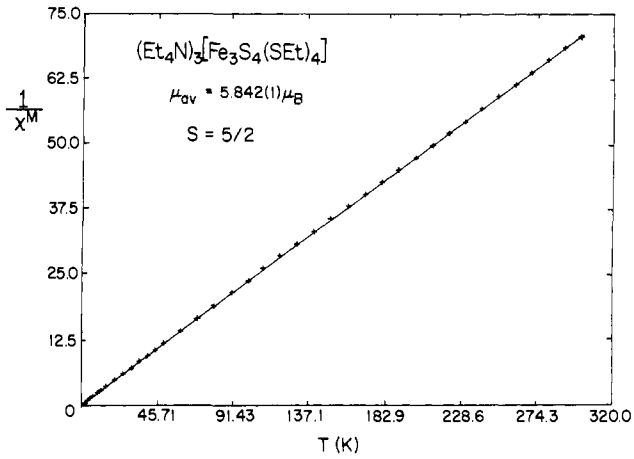

Figure 2. Plot of the temperature dependence of the reciprocal of the molar magnetic susceptibility (cgsu/mol) of polycrystalline $(Et_4N)_3[Fe_3S_4(SEt)_4]$ at H_0 = 5.00 kOe. The solid line is a fit to eq 1 at 5.00–300.3 K with the parameters in eq 1.

In our search for synthetic analogues of protein Fe_3S_4 sites, we have isolated Et_4N^+ salts of the clusters $[Fe_3S_4(SR)_4]^{3-}$ (R = Et, Ph) and shown them to have the linear structure **3**.[23] Certain bond distances and angles of $[Fe_3S_4(SPh)_4]^{3-}$, averaged under D_{2d} symmetry, are given in Figure 1. Previously, we have noted briefly that the EPR spectra of $[Fe_3S_4(SEt)_4]^{3-}$ ($g \sim 4.2$) and oxidized protein sites ($g \sim 2.0$) are different.[23b] This has the useful consequence of directly eliminating **3** as the structure of any currently recognized protein Fe_3S_4 site. It does not, of course, remove the viability of **3** as a possible site structure in other cases. For this reason, and to document differences between linear clusters and Fe_3S_4 sites and provide electronic structural criteria of the former, we present here an account of the magnetic and Mössbauer spectroscopic properties of $[Fe_3S_4(SR)_4]^{3-}$. These clusters are of substantial interest in their own right for the $[Fe_3S_4]^+$ core is a solubilized fraction of the extended chain structures of $KFeS_2$ and $CsFeS_2$,[29] which are linear antiferromagnets.[30] No Fe–S clusters of types **1** and **2** have yet been synthesized.

Experimental Section

Preparation of Compounds. $(Et_4N)_3[Fe_3S_4(SR)_4]$ with R = Et and Ph were prepared as previously described.[23b] Samples used in physical measurements had absorption and ^1H NMR spectra identical with those of analytical samples.[23b] By magnetic susceptibility and Mössbauer spectroscopic criteria preparations of the R = Et compound were slightly purer.

Physical Measurements. All samples were prepared and all measurements were performed under anaerobic conditions. Magnetic susceptibility measurements were carried out on a SHE 905 SQUID Magnetometer. The samples (30–40 mg) were weighed and sealed in previously calibrated containers. Several runs with different containers and different samples of the same compound were made in order to ensure the reproducibility of the results. Diamagnetic corrections were applied by using values from a standard source.[31] Magnetization measurements to 86 kOe at 4.2 K were made with a vibrating sample magnetometer. Mössbauer spectral measurements were made with a conventional constant-acceleration spectrometer equipped with a ^{57}Co source in a rhodium matrix maintained at the same temperature as the absorber. Spectra were measured in zero field at 4.2 and 77 K and in applied magnetic fields up to 80 kOe at 4.2 K. Polycrystalline and solution samples were prepared as previously described.[32] Measurements in applied fields were

(20) Robbins, A. H.; Stout, C. D.; Piszkiewicz, D.; Gawron, O.; Yoo, C.-S.; Wang, B.-C.; Sax, M. *J. Biol. Chem.* **1982**, *257*, 9061.
(21) (a) Stout, C. D. In "Metal Ions in Biology"; Spiro, T. G., Ed.; Wiley-Interscience: New York, 1982; Vol. 4, Chapter 3. (b) Carter, C. W., Jr. In "Iron-Sulfur Proteins"; Lovenberg, W., Ed.; Academic Press: New York, 1977; Vol. III, Chapter 6.
(22) Berg, J. M.; Holm, R. H. In "Metal Ions in Biology"; Spiro, T. G., Ed.; Wiley-Interscience: New York, 1982; Vol. 4, Chapter 1.
(23) (a) Hagen, K. S.; Holm, R. H. *J. Am. Chem. Soc.* **1982**, *104*, 5496. (b) Hagen, K. S.; Watson, A. D.; Holm, R. H. *Ibid.* **1983**, *105*, 3905.
(24) (a) Christou, G.; Sabat, M.; Ibers, J. A.; Holm, R. H. *Inorg. Chem.* **1982**, *21*, 3518. (b) Henkel, G.; Strasdeit, H.; Krebs, B. *Angew. Chem., Int. Ed. Engl.* **1982**, *21*, 201.
(25) Holm, R. H.; Hagen, K. S.; Watson, A. D. In "Chemistry for the Future"; Grünewald, H., Ed.; Pergamon Press: New York, 1984, pp 115–124.
(26) A marginal exception is $[Fe_4S_4(SC_6H_4\text{-}o\text{-}OH)_4]^{2-}$, which in the crystalline state contains one FeS_4O coordination unit: Johnson, R. E.; Papaefthymiou, G. C.; Frankel, R. B.; Holm, R. H. *J. Am. Chem. Soc.* **1983**, *105*, 7280. Two 5-coordinate Fe atoms are found in $[Fe_4S_4(SPh)_2(S_2CNEt_2)_2]^{2-}$ which, however, contains two non-thiolate ligands: Kanatzidis, M. G.; Ryan, M.; Coucouvanis, D.; Simopoulos, A.; Kostikas, A. *Inorg. Chem.* **1983**, *22*, 179.
(27) Bruschi, M. *Biochem. Biophys. Res. Commun.* **1979**, *91*, 623.
(28) Rydén, L.; Öfverstedt, L.-G.; Beinert, H.; Emptage, M. H.; Kennedy, M. C. *J. Biol. Chem.* **1984**, *259*, 3141.
(29) (a) Boon, J. W.; MacGillavry, C. H. *Recl. Trav. Chim. Pays-Bas* **1942**, *61*, 910. (b) Bronger, W. *Z. Anorg. Allg. Chem.* **1968**, *359*, 225.
(30) Sweeney, V. W.; Coffman, R. E. *Biochim. Biophys. Acta* **1972**, *286*, 26.
(31) Landolt-Bornstein, "Numerical Data and Functional Relationships in Science and Technology"; König, E., Ed.; Springer-Verlag: Berlin, 1966; Vol. II-2, "Magnetic Properties of Coordination and Organometallic Transition Metal Compounds".

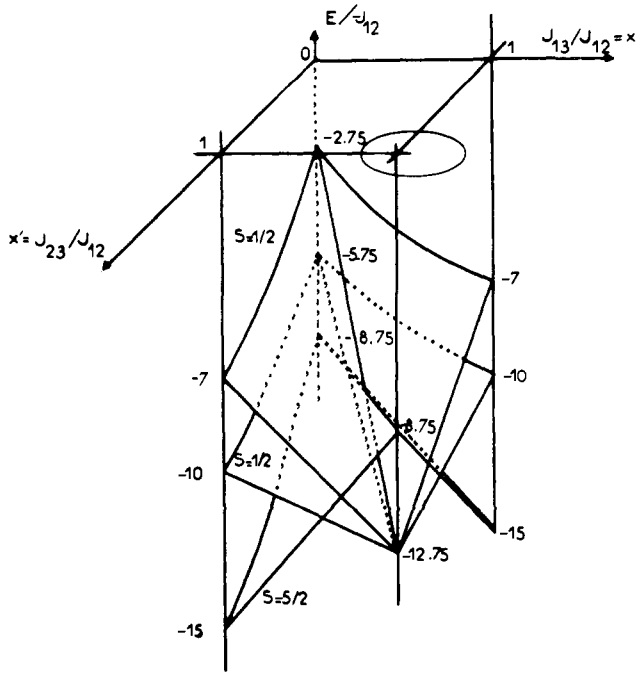

Figure 3. Schematic representation of the energy surfaces of the lowest states of a system containing three antiferromagnetically coupled $S = {}^5/_2$ sites, plotted as a function of the parameters x and x'. Planes referred to in the text are perpendicular to the x and x' axes at $x = 1$ and $x' = 1$, respectively, and the diagonal plane is defined by the E axis and the $x = x'$ line in the x, x' plane.

also made on powdered samples dispersed in Nujol mulls. Spectra were the same as those of polycrystalline samples. Cluster concentrations in solution samples were ~70 mM. Isomer shifts are referenced to Fe metal at room temperature.

Results

Magnetism. The magnetic susceptibility of polycrystalline $(Et_4N)_3[Fe_3S_4(SEt)_4]$ was examined at 5–300 K in fields H_0 = 0.5–40 kOe. Results were slightly field dependent. Those obtained at H_0 = 5 kOe are plotted in Figure 2. The data conform to the Curie–Weiss law (eq 1); parameters C and θ were evaluated from linear regression analysis. The magnetic moments $\mu = 2.828$

$$1/\chi^M = (T - \theta)/C \quad (1)$$

$$C = 4.268 \pm 0.002 \text{ emu K/mol}$$

$$\theta = -0.58 \pm 0.08 \text{ K}$$

$$\mu_{av} = 5.842 \pm 0.001\ \mu_B$$

$[\chi^M(T - \theta)]^{1/2}$ were calculated at some 40 points in the interval 5.00–300.3 K. The average value of the magnetic moment is close to the value of 5.92 μ_B, the spin-only moment of an $S = {}^5/_2$ state. With the near-zero value of θ, these results establish that $[Fe_3S_4(SEt)_4]^{3-}$ has a spin sextet ground state. Similar measurements have established the same state for $[Fe_3S_4(SPh)_4]^{3-}$. For the former cluster below ~50 K, deviations from the Curie law (eq 1, $\theta = 0$) become evident. The magnetization of $[Fe_3S_4(SEt)_4]^{3-}$ at 4.2 K deviates slightly from a Brillouin function dependence on the applied field in approaching the saturation value of $\mu = gS = 5\ \mu_B$ per cluster. At 80 kOe the magnetic moment per cluster is 4.73 μ_B.

Isomer shifts and quadrupole splittings of $[Fe_3S_4(SEt)_4]^{3-}$, discussed in a following section, are consistent with three high-spin Fe(III) atoms. Thus, individual iron spins $S_i = {}^5/_2$ combine to produce a total spin $|\vec{S}| = |\vec{S}_1 + \vec{S}_2 + \vec{S}_3| = {}^5/_2$. Systems of three coupled high-spin Fe(III) sites have been studied theoretically[33-36]

Table I. Spin States of Three Coupled High-Spin Fe(III) Sites

S	no.	S	no.
$^{15}/_2$	1	$^7/_2$	5
$^{13}/_2$	2	$^5/_2$	6
$^{11}/_2$	3	$^3/_2$	4
$^9/_2$	4	$^1/_2$	2

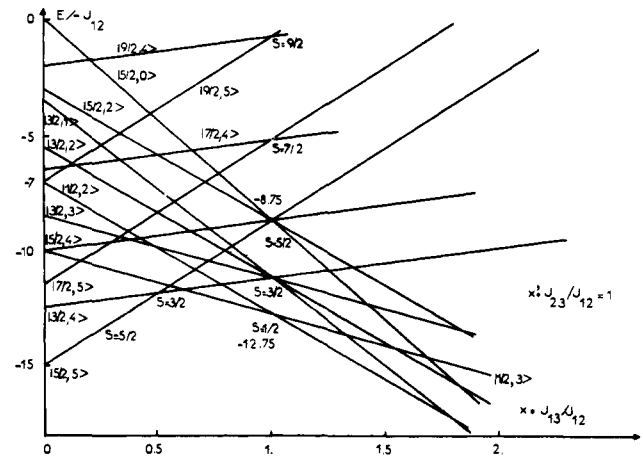

Figure 4. Energy levels of the states $|S,S'\rangle$ of a system containing three antiferromagnetically coupled $S = {}^5/_2$ sites, plotted as a function of x at $x' = 1$.

and examined experimentally[4,8,11,13,15,36,37] by measurement of magnetic susceptibility, EPR spectra, and Mössbauer spectra. We provide here a brief theoretical treatment of the spin-energy spectrum of three antiferromagnetically coupled $S = {}^5/_2$ sites. The treatment is related to those of Kent et al.[34] and Gayda et al.,[13] but it is elaborated in the form of graphical presentation of results showing clearly how different ground states arise as a consequence of different relative values of the exchange interaction constants J_{ij}.

The spin-dependent part of the interaction between the three magnetic sites 1, 2, 3 is expressed by the Heisenberg exchange Hamiltonian (eq 2). The eigenvalue problem for the general case

$$\mathcal{H}_{ex} = -J_{12}\vec{S}_1\cdot\vec{S}_2 - J_{23}\vec{S}_2\cdot\vec{S}_3 - J_{13}\vec{S}_1\cdot\vec{S}_3 \quad (2)$$

of three different J values can be solved by diagonalizing H_{ex} in the basis of product states of individual Fe(III) sites $|S_1M_1\rangle|S_2M_2\rangle|S_3M_3\rangle$, where $S_i = {}^5/_2$ and $-{}^5/_2 \le M_i \le {}^5/_2$. The eigenvalue problem has been solved by Griffith.[33] The energy surfaces of the lowest states of the antiferromagnetically coupled system ($J_{ij} < 0$) are schematically represented in the three-dimensional plot of Figure 3. Here we use the notation of eq 3 and 4. From the structure of cluster **3** (Figure 1), it is expected

$$\mathcal{H}_{ex}/-J_{12} = \vec{S}_1\cdot\vec{S}_2 + x\vec{S}_1\cdot\vec{S}_3 + x'\vec{S}_2\cdot\vec{S}_3 \quad (3)$$

$$x = J_{13}/J_{12} \text{ and } x' = J_{23}/J_{12} \quad (4)$$

$$\mathcal{H}_{ex}/-J = \vec{S}_2\cdot(\vec{S}_1 + \vec{S}_3) + x\vec{S}_1\cdot\vec{S}_3 \quad (5)$$

that $J_{12} = J_{23} = J$. Equation 2 can be rewritten as eq 5. For this case, unlike that of three unequal J values, the eigenvalue problem can be solved analytically. We assume that $\vec{S}_1$ and $\vec{S}_3$ couple to produce a spin $\vec{S}'$, which couples with $\vec{S}_2$ to form the total spin S of the cluster; i.e., $\vec{S}' = \vec{S}_1 + \vec{S}_3$ and $\vec{S} = \vec{S}' + \vec{S}_2$. The 27 spin states and their occurrence numbers, obtained in this way, are

(32) Laskowski, E. J.; Reynolds, J. G.; Frankel, R. B.; Foner, S.; Papaefthymiou, G. C.; Holm, R. H. *J. Am. Chem. Soc.* **1979**, *101*, 6562.
(33) Griffith, J. S. *Struct. Bonding (Berlin)* **1972**, *10*, 87.
(34) Kent, T. A.; Huynh, B. H.; Münck, E. *Proc. Natl. Acad. Sci. U.S.A.* **1980**, *77*, 6574.
(35) Fainzil'berg, V. E.; Belinskiĭ, M. I.; Tsukerblatt, B. S. *Sov. Phys.-JETP (Engl. Transl.)* **1980**, *52*, 314.
(36) (a) Hatfield, W. E. In "Theory and Applications of Molecular Paramagnetism"; Boudreaux, E. A., Mulay, L. N., Ed.; Wiley-Interscience: New York, 1976; Chapter 7 and references therein. (b) Ginsberg, A. P. *Inorg. Chim. Acta, Rev.* **1971**, *5*, 45.
(37) (a) Takano, M. *J. Phys. Soc. Jpn.* **1972**, *33*, 1312. (b) Yablokov, Y. V.; Gaponenko, V. A.; Zelentsov, V. V.; Suvorova, K. M. *Solid State Commun.* **1974**, *14*, 131. (c) Dziobkowski, C. T.; Wrobleski, J. T.; Brown, D. B. *Inorg. Chem.* **1981**, *20*, 671 and references therein.

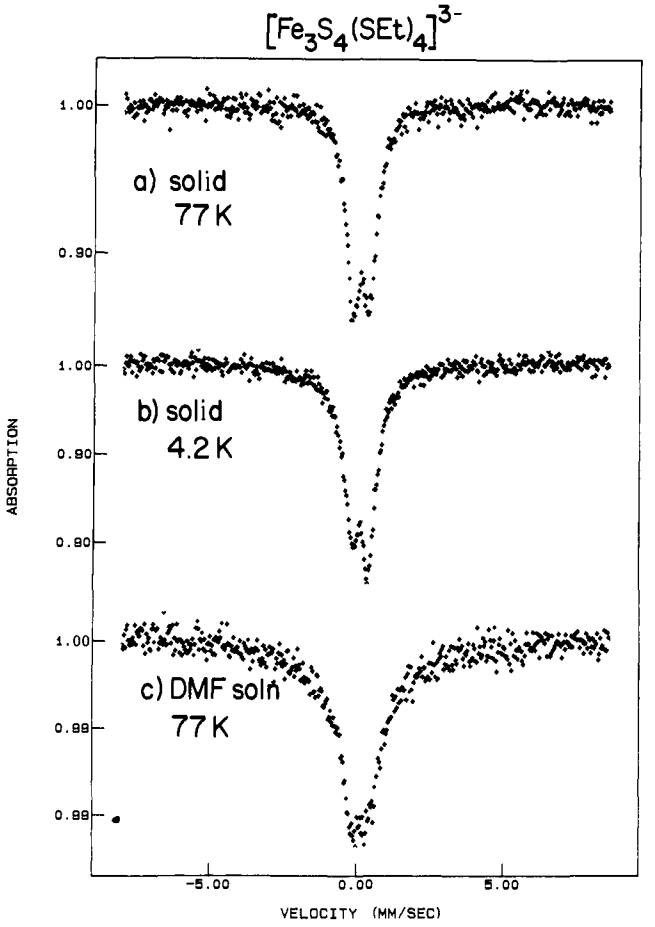

Figure 5. Mössbauer spectra of polycrystalline $(Et_4N)_3[Fe_3S_4(SEt)_4]$ at (a) 77 K and (b) 4.2 K and (c) a 70 mM solution in DMF at 77 K. At 4.2 K the solution spectrum shows incipient hyperfine splitting.

listed in Table I. Equation 5 can be expressed in the form of eq 6. This Hamiltonian is diagonal in S, S' and in S_1, S_2, and

$$\mathcal{H}_{ex}/-J = (1/2)[\vec{S}^2 - \vec{S}'^2 - \vec{S}_2^2] + (x/2)[\vec{S}'^2 - \vec{S}_1^2 - \vec{S}_3^2] \quad (6)$$

S_3. The eigenvalues are given by

$$E/-J = (1/2)[S(S+1) - S'(S'+1) - S_2(S_2+1)] + (x/2)[S'(S'+1) - S_1(S_1+1) - S_3(S_3+1)] \quad (7)$$

Since $S_i = {}^5/_2$, $S_i(S_i+1) = {}^{35}/_4$ and eq 7 becomes

$$E(S,S')/-J = (1/2)[S(S+1) - S'(S'+1) - 35/4] + (x/2)[S'(S'+1) - 35/2] \quad (8)$$

where S and S' take the values

$$|S_1 - S_3| < S' < S_1 + S_3 \qquad |S' - S_2| < S < S' + S_2 \quad (9)$$

In Figure 3 eq 8 defines the straight lines in the plane perpendicular to the x' axis at $x' = 1$. Plotted in Figure 4 is the energy level diagram for the low-lying eigenstates $|S,S'\rangle$ obtained by evaluating eq 8 for all allowable values of S and S' as a function of x. For $x \leq 0.5$ the ground state is $|{}^5/_2,5\rangle$. This is consistent with the magnetic moment of $[Fe_3S_4(SEt)_4]^{3-}$.

Calculation of the magnetic susceptibility[33] in the temperature range $T \gtrsim 50$ K showed that the experimental results could be reasonably simulated with the $S = {}^5/_2$ ground state and the parameters $g = 2$, $J = -300$ cm^{-1}, and $-100 \lesssim J_{13} \lesssim 100$ cm^{-1}. This supports the presence of antiferromagnetic coupling between adjacent Fe(III) sites, but the fits are of insufficient quality to fix either the sign or magnitude of J_{13}/J. For $T \lesssim 50$ K, $\chi^M T$ decreases with decreasing temperature, indicating a zero-field splitting of the $S = {}^5/_2$ manifold. The magnitude of the zero-field splitting parameter $|D| \lesssim 1$ cm^{-1} was obtained from a fit of the high-field magnetization to the Hamiltonian (eq 10), with the value of $E/D = 0.33$ taken from solution EPR measurements.[23b]

$$\mathcal{H} = g\beta\vec{H}_0\cdot\vec{S} + D[S_z^2 - (1/3)S(S+1)] + E[S_x^2 - S_y^2] \quad (10)$$

Table II. Mössbauer Spectral Data for $(Et_4N)_3[Fe_3S_4(SR)_4]$ at 77 K

R	δ,[a] mm/s	ΔE_Q,[b] mm/s	Γ,[c] mm/s
Et			
solid	0.23	0.52	0.60
DMF soln	0.25	0.55	0.72
Ph			
solid	0.29	0.63	0.68
DMF soln	0.24	0.60	0.72

[a] Relative to Fe metal at room temperature; ±0.03. [b] ±0.05. [c] ±0.04.

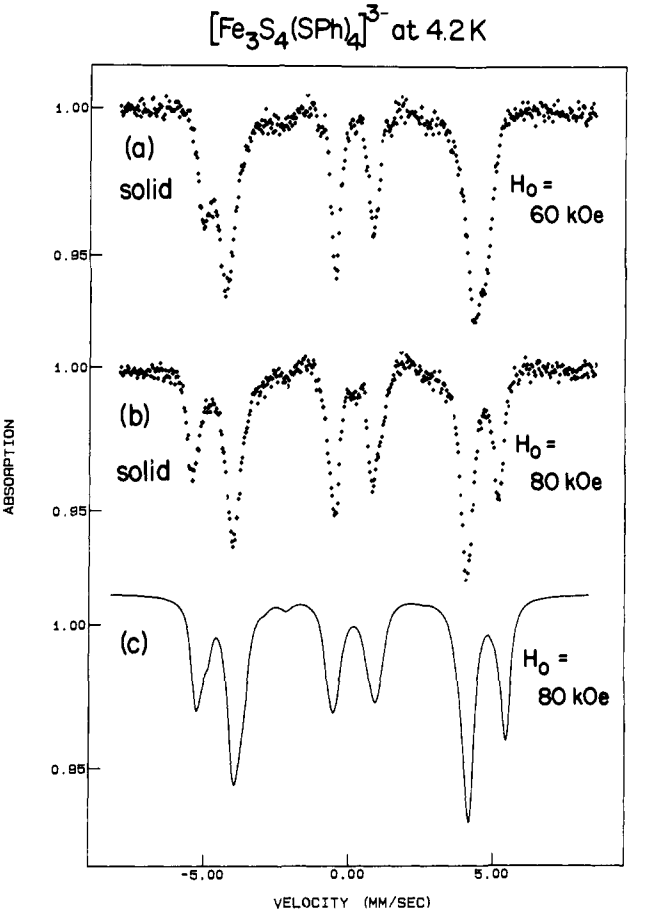

Figure 6. Mössbauer spectra of polycrystalline $(Et_4N)_3[Fe_3S_4(SPh)_4]$ at 4.2 K and (a) $H_0 = 60$ kOe and (b) $H_0 = 80$ kOe. (c) Simulation of spectrum b with $H_n = 310$ kOe, $\Delta E_Q = -0.60$ mm/s, and $\Gamma = 0.32$ mm/s for the lower intensity subspectrum and $H_n = 230$ kOe, $\Delta E_Q = -0.60$ mm/s, and $\Gamma = 0.44$ mm/s for the higher intensity subspectrum; $\eta = 0$ for both sites. The two subspectra have a 1:2 intensity ratio. A small contribution of a diamagnetic impurity was subtracted from the experimental spectra.[40]

Mössbauer Spectra. The compounds $(Et_4N)_3[Fe_3S_4(SR)_4]$ (R = Ph, Et) were examined at 4.2 and 77 K in the solid and solution states and in zero and applied longitudinal magnetic fields $H_0 \leq 80$ kOe. Isomer shifts (δ), quadrupole splittings (ΔE_Q), and line widths (Γ) are collected in Table II. Spectra of the two clusters are presented in Figures 5–7. For both clusters a broadened quadrupole doublet is observed at 77 K (Figure 5) indicative of inequivalent Fe sites, and at 4.2 K line broadening, apparently due to spin relaxation effects, is found and is more pronounced in solution samples. Values of δ and ΔE_Q are consistent with those of high-spin $Fe^{III}S_4$ for the three sites.[38,39] The close resemblance

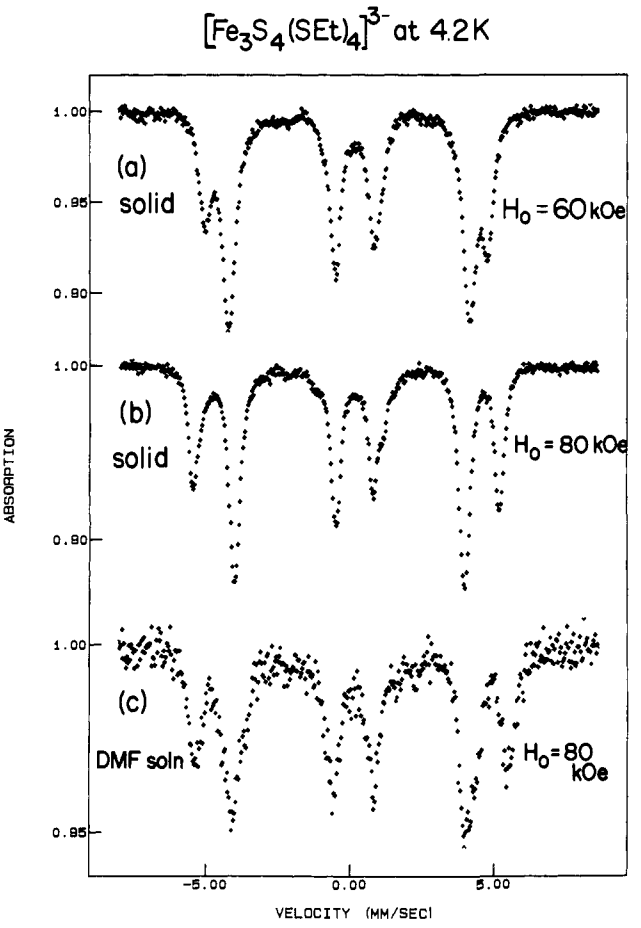

Figure 7. Mössbauer spectra of polycrystalline $(Et_4N)_3[Fe_3S_4(SEt)_4]$ at 4.2 K and (a) H_0 = 60 kOe and (b) H_0 = 80 kOe and a 70 mM solution in DMF at (c) H_0 = 80 kOe.

of the solid state and DMF solution spectra of $[Fe_3S_4(SEt)_4]^{3-}$ in Figure 7 provides convincing evidence for the retention of structure **3** in solution. A similar result has been found for $[Fe_3S_4(SPh)_4]^{3-}$.

Longitudinal magnetic fields at 4.2 K induce large magnetic fields at the Fe sites of the clusters. For $H_0 \geq 60$ kOe the $\Delta m = 0$ lines approach zero intensity, showing that the magnetic moment of the cluster is oriented parallel to the applied field. The spectra in Figures 6[40] and 7 are clearly resolved into two subspectra with relative intensities 1:2. For the higher intensity subspectrum the total field at the nucleus $\vec{H}_n = \vec{H}_0 + \vec{H}_{hf}$, which is the sum of the applied and magnetic hyperfine fields, decreases with increasing H_0, indicating a magnetic hyperfine interaction of negative sign for those Fe atoms. From the opposite observation, the magnetic hyperfine interaction for the Fe atom of the lower intensity subspectrum is positive.

A satisfactory simulation of the 80-kOe spectrum of polycrystalline $(Et_4N)_3[Fe_3S_4(SPh)_4]$ is shown in Figure 6c. The result yields $\Delta E_Q \cong -0.60$ mm/s for both sites. An average over the angle between the electric field gradient (efg) component V_{zz} and H_0 was taken to simulate the polycrystalline nature of the absorber. The broader widths of the features of the higher intensity subspectrum reflects some inequivalence between sites 1 and 3. The observed H_n values correspond to the hyperfine fields,

$$H_{hf_2} = +230 \pm 5 \text{ kOe} \qquad H_{hf_{1,3}} = -310 \pm 5 \text{ kOe} \tag{11}$$

The variation of H_{hf} with H_0 for the two subsites is shown in Figure 8. At H_0 = 80 kOe values of H_{hf} approach the maximum (saturation) values corresponding to complete polarization of the electron spin.

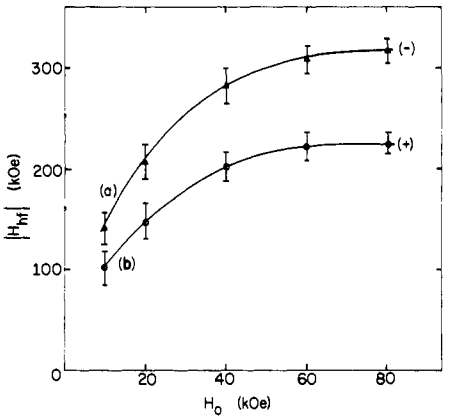

Figure 8. Values of H_{hf} at the two magnetic subsites as a function of the applied field H_0; (+) and (−) indicate that H_{hf} is parallel and antiparallel, respectively, to H_0.

The spectra of $[Fe_3S_4(SEt)_4]^{3-}$ in Figure 7 are sufficiently similar to those of $[Fe_3S_4(SPh)_4]^{3-}$ in Figure 6 to demonstrate that the two clusters are electronically analogous. There are, however, some differences. In the former case, the outer absorption lines of the majority spin component have the same width, possibly indicating larger asymmetry in the efg tensor ($\eta \sim 1$). Another possibility is crystallographic distortions at sites 1 and 3 which result in axial efg's of approximately equal magnitude but with principal components of opposite sign. In solution, the outer absorption lines have unequal widths, indicating axial efg's with principal components of negative sign for sites 1 and 3, as well as for site 2.

The magnetic field dependence of the Mössbauer spectrum of $[Fe_3S_4(SR)_4]^{3-}$ can be understood in terms of antiparallel exchange coupling of three high-spin Fe(III) sites. Neglecting the isomer shift and quadrupole splitting, the Mössbauer spectrum can be generated from the Hamiltonian of eq 12 in which the first term

$$\mathcal{H} = \sum_{i=1}^{3} (g\beta\vec{H}_0\cdot\vec{S}_i - g_n\beta_n\vec{H}_0\cdot\vec{I}_i + a_i\vec{I}_i\cdot\vec{S}_i) + H_{ex} \tag{12}$$

includes the electronic and nuclear Zeeman interactions and the magnetic hyperfine interaction. All interactions are treated as isotropic. The dominant term is H_{ex} (eq 2), and it results in an $S = {}^5/_2$ ground state. The Zeeman and magnetic hyperfine interactions can be evaluated in terms of this ground state. The appropriate part, eq 13, of the complete Hamiltonian contains

$$\mathcal{H}' = g\beta\vec{H}_0\cdot\langle\vec{S}\rangle - g_n\beta_n\sum_i\vec{H}_0\cdot\vec{I}_i + \sum_i A_i\vec{I}_i\cdot\langle\vec{S}\rangle \tag{13}$$

$\langle\vec{S}\rangle$, the expectation value of the total spin S, and A_i, the hyperfine interaction constant for the ith atom in the total spin representation. That is,

$$\sum_i a_i\vec{I}_i\cdot\vec{S}_i = \sum_i A_i\vec{I}_i\cdot\langle\vec{S}\rangle \tag{14}$$

Combining the last terms of eq 13 gives

$$\mathcal{H}' = g\beta\vec{H}_0\cdot\langle\vec{S}\rangle - g_n\beta_n\sum_i\vec{I}_i\cdot(\vec{H}_0 - A_i\langle\vec{S}\rangle/g_n\beta_n) \tag{15}$$

or

$$\mathcal{H}' = g\beta\vec{H}_0\cdot\langle\vec{S}\rangle - g_n\beta_n\sum_i\vec{I}_i\cdot\vec{H}_n \tag{16}$$

where the total magnetic field at the ith nucleus is given by

(38) Gillum, W. O.; Frankel, R. B.; Foner, S.; Holm, R. H. *Inorg. Chem.* **1976**, *15*, 1095. S_2-*o*-xyl = *o*-xylene-α,α'-dithiolate.

(39) Lane, R. W.; Ibers, J. A.; Frankel, R. B.; Papaefthymiou, G. C.; Holm, R. H. *J. Am. Chem. Soc.* **1977**, *99*, 84.

(40) In spectra of polycrystalline $(Et_4N)_3[Fe_3S_4(SPh)_4]$, a minority component (12% of the total intensity) was observed, for which the outer line splitting was equal to the applied field. The outer lines appeared at about +1.6 and −1.3 mm/s. The impurity has an $S = 0$ ground state and is most likely $[Fe_2S_2(SPh)_4]^{2-}$. On the basis of this assumption, the impurity spectrum was calculated by using known parameters of this species[38] and was numerically subtracted from spectra a and b of Figure 6. No impurity contributions were found in spectra of $(Et_4N)_3[Fe_3S_4(SEt)_4]$ preparations.

$$\vec{\mathcal{H}}_{n_i} = \vec{H}_0 - \frac{A_i(\vec{S})}{g_n\beta_n} = \vec{H}_0 + \vec{H}_{hf_i} \quad (17)$$

Because the intensity of the $\Delta m = 0$ lines approaches zero in the high-field spectra, the induced spin is parallel to the applied field (taken as the z direction), i.e., $\langle\vec{S}_x\rangle = \langle\vec{S}_y\rangle = 0$, and, therefore,

$$\vec{\mathcal{H}}_{hf_i} = -A_i\langle\vec{S}_z\rangle/g_n\beta_n \quad (18)$$

For a comparison of experimental values of hyperfine interaction constants with such quantities in related molecules, the constants a_i are calculated. These correspond to the projection of the spin of the ith Fe(III) atom on the z axis, $\langle S_{iz}\rangle$. From eq 13,

$$a_i\langle S = {}^5/_2, S_z|S_{iz}|S = {}^5/_2, S_z\rangle = A_i\langle S = {}^5/_2, S_z|S_z|S = {}^5/_2, S_z\rangle \quad (19)$$

or

$$a_i = A_i\langle S_z\rangle/\langle S_{iz}\rangle \quad (20)$$

The left side of eq 19 can be evaluated by expanding the total spin wave function in terms of product states of the individual Fe(III) atoms with use of the usual angular momentum coupling rules.[41] The contributing states and their relative weights in the total spin state $|S = {}^5/_2, S_z = {}^5/_2\rangle$ are listed in Table III.[42] Values of the ratio $\langle S_z\rangle/\langle S_{iz}\rangle$ for $i = 1, 2, 3$ can then be calculated. We obtain $\langle S_{1z}\rangle = \langle S_{3z}\rangle = 2.14$ and $\langle S_{2z}\rangle = -1.79$; hence

$$a_i = 1.168A_i\ (i = 1, 3) \qquad a_i = -1.400A_i\ (i = 2) \quad (21)$$

Because the exchange interactions are isotropic, these values are the same for all other S_z states in the manifold. With use of the observed H_{hf} values, the constants A_i can be calculated from eq 18 with $\langle S_z\rangle = -2.36$, obtained from the magnetization at 80 kOe and 4.2 K. Then values of a_i can be evaluated from eq 21, giving

$$\begin{aligned} a_i/g_n\beta_n &= -153 \pm 3 \text{ kOe/spin } (i = 1, 3) \\ a_i/g_n\beta_n &= -137 \pm 3 \text{ kOe/spin } (i = 2) \end{aligned} \quad (22)$$

Discussion

The spin-state energy spectrum of a system containing three high-spin antiferromagnetically coupled Fe(III) atoms is a sensitive function of the exchange parameters J_{ij}. Thus the two $S = {}^1/_2$ states in the plane perpendicular to the x' axis at $x' = 1$ in Figure 3 decrease, and the $S = {}^5/_2$ state increases, in energy as the ratio x (eq 4) increases from 0 to 1. The same behavior holds for these states in the plane perpendicular to the x axis at $x = 1$ as $x' = 0 \rightarrow 1$. When the three coupling constants of eq 2 are equal ($x = x' = 1$), the energies are given by

$$E/-J = S(S + 1)/2 - 105/8 \quad (23)$$

In this case, states with the same spin S are degenerate, as shown by convergence of the $S = {}^1/_2$ state energies at the value −12.75. In the plane $x = x'$ the energies of the two $S = {}^1/_2$ states, at −2.75 and −5.75 when $x = x' = 0$, decrease to −12.75 at $x = x' = 1$ while the energy of the lowest $S = {}^5/_2$ state is constant at −8.75. The energies of states at positions not intersected by the aforementioned plane can be calculated by using the matrices given by Griffith.[33]

As already observed, the experimental ground state $|{}^5/_2, 5\rangle$ for $[Fe_3S_4(SR)_4]^{3-}$ obtains in the domain $x' = 1$, $x < 0.5$ of Figure 3. Given in Figure 4 is a more complete representation of the lowest spin states in the plane perpendicular to the x' axis at $x' = 1$, which is the appropriate approximation for $J_{12} = J_{23}$.[43] As x is increased, several discontinuities in ground-state S occur. There is a brief range of stability of an $S = {}^3/_2$ state above $x = 0.5$, and then $S = {}^1/_2$ state(s) become lowest at $0.6 \lesssim x \lesssim 1.8$. The important point emerging from this analysis, as well as from that of Kent et al.,[34] is that in order to have an $S = {}^1/_2$ ground state the three J_{ij} must not be too different, a matter conveyed by the circle around the $x = x' = 1$ point in Figure 3. Conversely, an $S = {}^5/_2$ ground state will exist only if the ratio x or x' is small. The estimated value $J_{12} = J_{23} = -300$ cm^{-1} compares well with the experimental values of $[Fe_2S_2(S_2\text{-}o\text{-xyl})_2]^{2-}$[38] (−300 cm^{-1}), $[Fe_2S_2Cl_4]^{2-}$[44] (−316 cm^{-1}), $KFeS_2$[30] (ca. −400 cm^{-1}), and $[Fe_2S_2]^{2+}$ sites of ferredoxins[45,46] (ca. −370 cm^{-1}). These species contain $Fe_2(\mu_2\text{-S})_2$ units closely similar in structure to those in $[Fe_3S_4(SPh)_4]^{3-}$.[23]

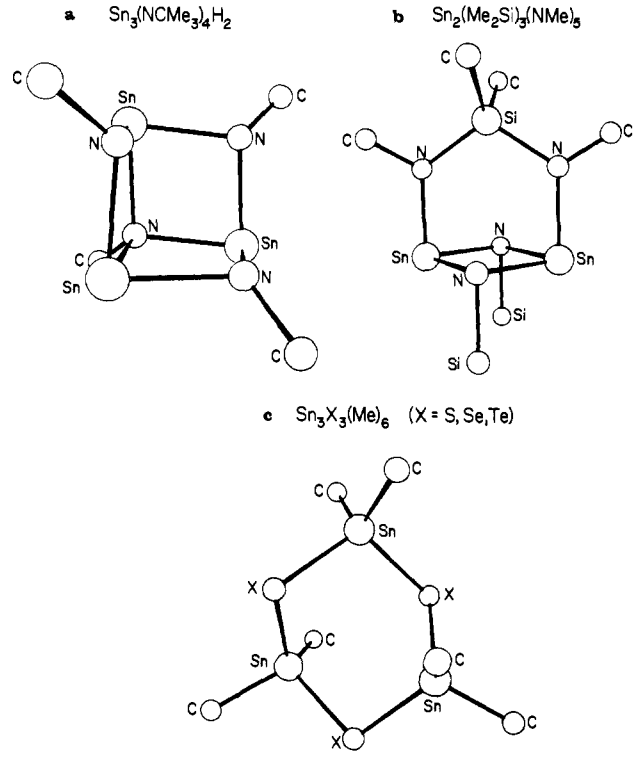

Figure 9. Depictions of the structures of (a) $Sn_3(NCMe_3)_4H_2$,[50] (b) $Sn_2(Me_2Si)_3(NMe)_5$,[51] and (c) $Sn_3X_3Me_6$.[53,54] Omitted are methyl groups on N and Si atoms, the two H atoms in part a, and the NMe group bridging the two lower $SiMe_2$ groups in part b. Structures a and c were produced from published coordinates.[51,53b]

With reference to **3** in Figure 1, Fe sites 1 and 3 with magnetic hyperfine constant −153 kOe/spin are of the type $FeS_2(SR)_2$. Site 2 with magnetic hyperfine constant −137 kOe/spin is of the type FeS_4. These constants are comparable with the values −162 kOe/spin for the $Fe(S\text{-Cys})_4$ site in oxidized rubredoxin[47] and −149 kOe/spin for the Fe(III) site in [2Fe-2S]$^+$ ferredoxins.[48]

Spectroscopic data for protein $[Fe_3S_4]^+$ sites indicate an $S = {}^1/_2$ ground state and Fe···Fe separations of ~2.7 Å.[2,12,17] As observed at the outset and documented fully here, the $S = {}^5/_2$ ground state and associated Mössbauer spectroscopic properties of $[Fe_3S_4(SR)_4]^{3-}$ eliminate the linear structure **3** as a synthetic analogue of these sites. This leaves clusters **1** and **2** as viable alternatives. Both could be configured to satisfy the condition $x \cong x'$ required for an $S = {}^1/_2$ ground state (Figures 3 and 4). In this respect the expected C_{3v} symmetry of **1** is especially attractive. The topology of this structure in the general form $M_3(\mu_3\text{-X})(\mu_2\text{-X})_3L_n$ with idealized trigonal symmetry has been

(41) Rotenberg, M.; Bivins, R.; Metropolis, N.; Wooten, J. K., Jr. "The 3-j and 6-j Symbols"; The Technology Press, Massachusetts Institute of Technology: Cambridge, MA, 1959.

(42) See the paragraph at the end of this article concerning supplementary material.

(43) These two values cannot be identical in $(Et_4N)_3[Fe_3S_4(SPh)_4]$ owing to small differences in the two $Fe_2(\mu_2\text{-S})_2$ bridge units, as reflected by the distances Fe(1)–Fe(2) = 2.703 (2) Å and Fe(2)–Fe(3) = 2.725 (2) Å.[23] The mean of these distances is given in Figure 1.

(44) Wong, G. B.; Bobrik, M. A.; Holm, R. H. *Inorg. Chem.* **1978**, *17*, 578.

(45) Palmer, G.; Dunham, W. R.; Fee, J. A.; Sands, R. H.; Iizuka, T.; Yonetani, T. *Biochim. Biophys. Acta* **1971**, *245*, 201.

(46) Petersson, L.; Cammack, R.; Rao, K. K. *Biochim. Biophys. Acta* **1980**, *622*, 18.

(47) Schultz, C. E.; Debrunner, P. G. *J. Phys. (Paris) Colloq.* **1979**, *37*, 154.

(48) Sands, R. H.; Dunham, W. R. *Q. Rev. Biophys.* **1975**, *7*, 443.

realized with a number of clusters.[49] The closest resemblance to **1** is found with three Mo_3S_4 complexes.[49b-d] Recent advances in Sn–N chemistry by Veith and co-workers[50-52] have provided topological equivalents of **1** and **2**, which are depicted in Figure 9. Here pyramidal Sn(II) and RN^{2-} simulate tetrahedral Fe(II,III) and S^{2-} atoms, respectively. The structure of $Sn_3(NCMe_3)_4H_2$ has been crystallographically established.[50] The two hydrogen atoms are presumably associated with the nitrogen atoms in the open face of the cage, but their positions have not been located. The structure of $Sn_2(Me_2Si)_3(NMe)_5$[51] is consistent with its ^1H NMR spectrum and the usual stereochemical preferences of the framework atoms. It has not been demonstrated by X-ray diffraction. The upper $SiMe_2$ group simulates $Fe(SR)_2$. The NMe bridge between the lower two $SiMe_2$ groups has been omitted to emphasize the topological similarity to **2**, especially **2a**. The set of compounds also includes cubane-like $Sn_4(NNMe_2)_4$[52] (not shown), similar to Fe_4S_4 clusters.[22] Topological approaches to the cyclic $[Fe_3S_3]^{3+}$ site in *Av* Fd I are provided by $Me_6Sn_3X_3$,[53,54] a point originally recognized by Ghosh et al.[3a]

Although the linear cluster **3** is not a representative of the 3-Fe site in the "native" form of any protein so far examined, it has been found under certain conditions in one protein. In an unfolded form of aconitase, obtained by incubation at pH >9.5, the linear structure has been identified by several methods,[55] including Mössbauer spectroscopy. Efforts to produce the nonlinear $[Fe_3S_4]^+$ unit by isomerization of **3** or other means continue in this laboratory. At present, the only property shared by the clusters $[Fe_3S_4(SR)_4]^{3-}$ and protein 3-Fe sites is the formation of the $[Fe_4S_4]^{2+}$ core when treated with Fe(II).[11,18,19,23b]

Acknowledgment. This research was supported at Harvard University by NIH Grant GM 28856, at M.I.T. by the National Science Foundation, and at the Lawrence Berkeley Laboratory by the Director, Office of Energy Research, Office of Basic Energy Sciences, Chemical Sciences Division of the U.S. Department of Energy under Contract No. DE-AC03-76SF00098. We thank J. M. Berg for the preparation of Figure 9 and for useful discussions, Professor H. Beinert for disclosure of results prior to publication, and Professor E. Münck for insightful commentary. We also thank Dr. S. Foner for help with the magnetization measurements.

Registry No. $(Et_4N)_3[Fe_3S_4(SEt)_4]$, 85647-20-7; $(Et_4N)_3[Fe_3S_4(SPh)_4]$, 82661-12-9.

Supplementary Material Available: Contributing states and relative weights in the total spin state $|S = {}^5/_2, S_z = {}^5/_2\rangle$, including a brief derivation of the results (3 pages). Ordering information is given on any current masthead page.

(49) (a) $(C_5H_5)_3Mn_3(NO)_4$: Elder, R. C.; Cotton, F. A.; Schunn, R. A. *J. Am. Chem. Soc.* **1967**, *89*, 3645. (b) $[(C_5H_5)_3Mo_3S_4]^+$: Vergamini, P. J.; Vahrenkamp, H.; Dahl, L. F. *Ibid.* **1971**, *93*, 6327. (c) $[Mo_3S_4(CN)_9]^{5-}$: Müller, A.; Reinsch, U. *Angew. Chem., Int. Ed. Engl.* **1980**, *19*, 72. (d) $[Mo_3S_4(SCH_2CH_2S)_3]^{2-}$: Halbert, T. R.; McGauley, K.; Pan, W.-H.; Czernuszewicz, R. S.; Stiefel, E. I. *J. Am. Chem. Soc.* **1984**, *106*, 1849. (e) $[W_3O_4F_9]^{5-}$: Mattes, R.; Mennemann, K. *Z. Anorg. Allg. Chem.* **1977**, *437*, 175. (f) $[Mo_3O_4(C_2O_4)_3(H_2O)_3]^{2+}$: Bino, A.; Cotton, F. A.; Dori, Z. *J. Am. Chem. Soc.* **1978**, *100*, 5252. (g) $[(Mo_3O_4)_2(EDTA)_3]^{4-}$: Bino, A.; Cotton, F. A.; Dori, Z. *Ibid.* **1979**, *101*, 3842. (h) $[Mo_3O_4(OAc)_3(H_2O)_3]^{2+}$: Bino, A.; Cotton, F. A.; Dori, Z. *Inorg. Chim. Acta* **1979**, *33*, L133. (i) $[Mo_3(OMe)_4(NO)_3(CO)_6]^-$: Kirtley, S. W.; Chanton, J. P.; Love, R. A.; Tipton, D. L.; Sorrell, T. N.; Bau, R. *J. Am. Chem. Soc.* **1980**, *102*, 3451. (j) $[Mo_3O_4(MeN(CH_2CO_2)_2)_3]^{2-}$: Gheller, S. F.; Hambley, T. W.; Brownlee, R. T. C.; O'Connor, M. J.; Snow, M. R.; Wedd, A. G. *Ibid.* **1983**, *105*, 1527.

(50) Veith, M. *Z. Naturforsch., B: Anorg. Chem., Org. Chem.* **1980**, *35B*, 20.

(51) Veith, M.; Grosser, M.; Rechtenwald, O. *J. Organomet. Chem.* **1981**, *216*, 27.

(52) Veith, M.; Schlemmer, G. *Chem. Ber.* **1982**, *115*, 2141.

(53) X = S: (a) Menzebach, B.; Bleckmann, P. *J. Organomet. Chem.* **1975**, *91*, 291. (b) Jacobsen, H.-J.; Krebs, B. *Ibid.* **1977**, *136*, 333.

(54) (a) X = Se: Dräger, M.; Blecher, A.; Jacobsen, H.-J.; Krebs, B. *J. Organomet. Chem.* **1978**, *161*, 319. (b) X = Te: Blecher, A.; Dräger, M. *Angew. Chem.* **1979**, *18*, 677.

(55) Kennedy, M. C.; Kent, T. A.; Emptage, M. H.; Merkle, H.; Beinert, H.; Münck, E. *J. Biol. Chem.*, in press.

Molecular Mechanics and Crystallographic Study of Hole Sizes in Nitrogen-Donor Tetraaza Macrocycles

Vivienne J. Thöm, Christine C. Fox, Jan C. A. Boeyens,* and Robert D. Hancock*

Contribution from the Department of Chemistry, University of the Witwatersrand, Johannesburg, South Africa 2001. *Received February 6, 1984*

Abstract: The preparation and crystal structure of [Cu(13-aneN_3O)Br]Br (compound I) (13-aneN_3O = 1-oxa-4,7,11-triazacyclotridecane) and of $[Ni(14\text{-ane}N_4)(NO_3)_2]$ (II) are reported, with *R* factors of 0.099 and 0.063 (14-aneN_4 = 1,4,8,11-tetraazacyclotetradecane). In I the complex cation consists of an approximately square-pyramidal arrangement, with the axial position occupied by a bromide ion and the Cu atom 0.47 Å above the plane formed by the donor atoms of 13-aneN_3O. In II the nitrate ions occupy the axial positions with long Ni–O lengths of 2.169 Å, while the mean Ni–N lengths are short, at 2.055 Å. Molecular mechanics (MM) calculations are used to determine best-fit sizes for metal ions fitting into tetraaza macrocycles in the trans-I and trans-III conformers. The MM calculations show that the trans-I conformer of 12-aneN_4 (1,4,7,10-tetraazacyclododecane) will be more stable in planar coordination than the trans-III form and that metal ions with M–N lengths of 2.11 Å will fit best into the trans-I form. The MM shows that for 13-aneN_4 (1,4,7,11-tetraazacyclotridecane) the best-fit M–N length for the trans-I form will be 2.03 Å, accounting for the adoption of this conformation by [Cu(13-aneN_3O)Br]$^+$, with Cu–N = 2.02 Å. The trans-III form has a best-fit size of 1.92 Å and is preferred by smaller metal ions. The best-fit M–N length for 14-aneN_4 in the trans-III conformation is 2.05 Å, while the trans-I will be more stable above 2.29 Å. Octahedral coordination would involve severe steric strain for trans-I conformers, and if octahedral coordination must be maintained, then the folded cis-V conformer is preferred at M–N lengths above 2.09 Å. The origin of the short Ni–N bond lengths in II is examined. The MM suggests that this is not due to compression by the macrocycle, but it is a consequence of the presence of the two axial oxygen atoms. The long Ni–O bonds are the result of steric repulsion by the hydrogen atoms on the macrocycle.

Many of the properties of the complexes of macrocycles appear to be controlled by the size of the cavity in the center of the macrocycle. Busch et al.[1] have calculated the best-fit metal–nitrogen (M–N) bond lengths for metal ions fitting into the cavities

0002-7863/84/1506-5947$01.50/0